The Journal of Immunology

TLR7- and TLR9-Responsive Human B Cells Share Phenotypic and Genetic Characteristics

Noa Simchoni and Charlotte Cunningham-Rundles

J Immunol 2015; 194:3035-3044; Prepublished online 4 March 2015;
doi: 10.4049/jimmunol.1402690
http://www.jimmunol.org/content/194/7/3035

The Journal of Immunology is published twice each month by
The American Association of Immunologists, Inc.,
1451 Rockville Pike, Suite 650, Rockville, MD 20852

Print ISSN: 0022-1767 Online ISSN: 1550-6606.

TLR7- and TLR9-Responsive Human B Cells Share Phenotypic and Genetic Characteristics

Noa Simchoni and Charlotte Cunningham-Rundles

B cells activated by nucleic acid–sensing TLR7 and TLR9 proliferate and secrete immune globulins. Memory B cells are presumably more responsive due to higher TLR expression levels, but selectivity and differential outcomes remain largely unknown. In this study, peripheral blood human B cells were stimulated by TLR7 or TLR9 ligands, with or without IFN-α, and compared with activators CD40L plus IL-21, to identify differentially responsive cell populations, defined phenotypically and by BCR characteristics. Whereas all activators induced differentiation and Ab secretion, TLR stimulation expanded IgM$^+$ memory and plasma cell lineage committed populations, and favored secretion of IgM, unlike CD40L/IL-21, which drove IgM and IgG more evenly. Patterns of proliferation similarly differed, with CD40L/IL-21 inducing proliferation of most memory and naive B cells, in contrast with TLRs that induced robust proliferation in a subset of these cells. On deep sequencing of the IgH locus, TLR-responsive B cells shared patterns of IgHV and IgHJ usage, clustering apart from CD40L/IL-21 and control conditions. TLR activators, but not CD40L/IL-21, similarly promoted increased sharing of CDR3 sequences. TLR-responsive B cells were characterized by more somatic hypermutation, shorter CDR3 segments, and less negative charges. TLR activation also induced long positively charged CDR3 segments, suggestive of autoreactive Abs. Testing this, we found culture supernatants from TLR-stimulated B cells to bind HEp-2 cells, whereas those from CD40L/IL-21–stimulated cells did not. Human B cells possess selective sensitivity to TLR stimulation, with distinctive phenotypic and genetic signatures. ***The Journal of Immunology*****, 2015, 194: 3035–3044.**

B cells are commonly activated by Ag and costimulated by CD40L and cytokines in germinal centers; however, B cells can also be activated by selected TLR agonists, leading to enhanced cell survival, proliferation, secretion of IL-6 and IL-10, isotype switch, and differentiation into Ig-producing plasma cells (PCs) (1–3). Naive human B cells express low levels of TLRs 1, 6, 7, 9, and 10, whereas CD27$^+$ memory B cells have increased receptor expression, especially of TLR7 and TLR9 (4) activated by ssRNA or by unmethylated CpG motifs from microbial DNA. For stimulation using TLR7 agonists, removal of plasmacytoid dendritic cells reduced Ig production, whereas the addition of IFN-α, a transcriptional upregulator of TLRs (1), restored Ig secretion, suggesting that IFN-α is important for TLR7-driven Ab production. IFN-α similarly boosted responses of naive B cells to TLR9 agonists (5). TLR9 stimulation of human B cells induced IgM$^+$ memory B cells to secrete anti-carbohydrate Abs of the IgM isotype (6, 7) and other IgM Abs of broad specificity (8). These human B cell responses thus resemble well-characterized responses of murine innate-like B populations, namely B1 and splenic marginal zone B cells, both of which respond to TLR stimulation with rapid and high-titer Ab secretion (9–11). Although human peripheral blood IgM$^+$ memory B cells are not directly analogous to noncirculating rodent B1 or marginal zone B cells (12, 13), TLR9 stimulation nevertheless induces this population to secrete anti-carbohydrate and polyspecific IgM, consistent with the reactivities of "natural" Abs (NAs) that may provide early protection against bacterial infections (11, 14).

Although memory B cells, and especially IgM$^+$ memory B cells, are activated by TLR triggers, how TLR-responsive B cells might differ from T cell–activated B cells, in terms of BCR structure, Ig isotype production, and Ab specificity, has remained undefined. In this study, we have examined the hallmarks of TLR-responsive human peripheral blood B cells from healthy donors, assessing the responding cell phenotypes, production of Ig isotypes, and BCR characteristics as determined by deep sequencing. As a contrast, we compared TLR-responding cells to B cells responding to CD40L and IL-21 costimulation, a mimic of the germinal center environment. We found that TLR7 and TLR9 activation expanded IgM$^+$ memory (CD27$^+$) and PC lineage committed (CD27^{hi}) populations (15), resulting in preferential IgM secretion, unlike CD40L/IL-21 stimulation, which activated IgM$^-$ memory and PC committed populations, and induced more equal IgM and IgG production. The BCRs of TLR-responsive B cells also shared patterns of IgHV and IgHJ usage, were more likely to have undergone somatic hypermutation (SHM), and had shorter CDR3 segments with a less negative charge, unlike CD40L/IL-21–activated cells that lacked these characteristics. TLR-activated B cells also produced HEp-2–reactive autoantibodies not seen after CD40L/IL-21 stimulation. Thus, increased TLR responsiveness may define a subset of B cells with unique biological capacities.

Materials and Methods

Blood and B cell isolation

Deidentified leukocyte concentrates were obtained from four healthy blood donors from the New York Blood Center. PBMCs were isolated from these by centrifugation over Ficoll-Paque (GE Healthcare, Uppsala, Sweden), and B cells were isolated by negative magnetic selection using the human B Cell Isolation Kit II (Miltenyi Biotec, San Diego, CA).

Division of Clinical Immunology, Department of Medicine, Icahn School of Medicine at Mount Sinai, New York, NY 10029

Received for publication October 22, 2014. Accepted for publication February 3, 2015.

This work was supported by the National Institutes of Health (Grants AI 1061093, AI-349 0860037, AI-1048693, T32-GM007280), the Jeffrey Modell Foundation, and a David S. Gottesman Immunology Chair.

Address correspondence and reprint requests to Dr. Charlotte Cunningham-Rundles, Division of Clinical Immunology, Department of Medicine, Icahn School of Medicine at Mount Sinai, 1425 Madison Avenue, New York, NY 10029. E-mail address: charlotte.cunningham-rundles@mssm.edu

The online version of this article contains supplemental material.

Abbreviations used in this article: FSC, forward scatter; NA, natural Ab; PC, plasma cell; SHM, somatic hypermutation.

www.jimmunol.org/cgi/doi/10.4049/jimmunol.1402690

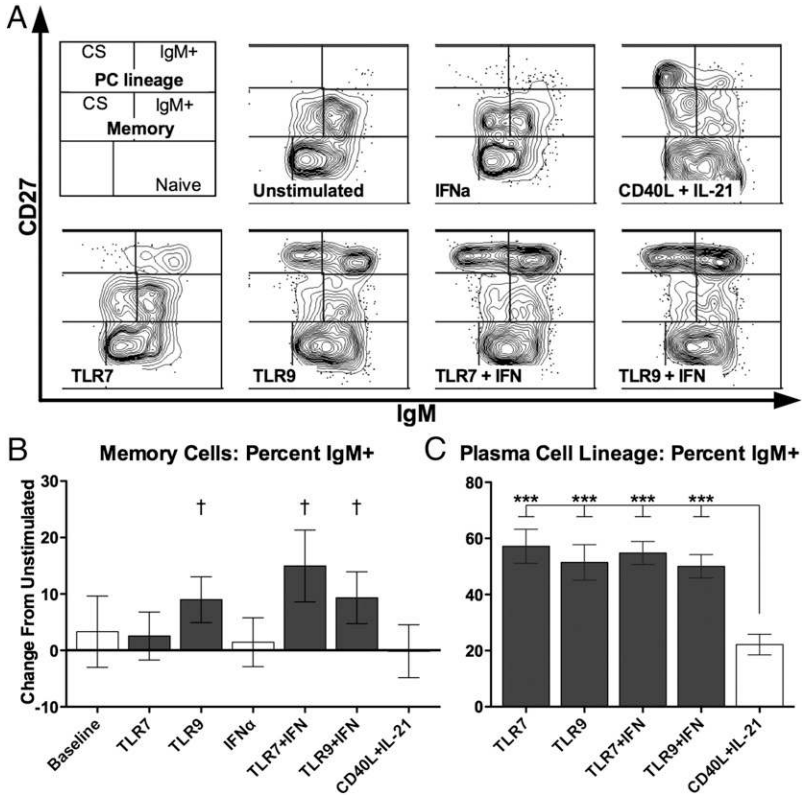

FIGURE 1. TLR stimulation of human B cells expands IgM$^+$ memory cells and PC lineage committed cells. (**A**) Representative day 7 cultured cells characterized by flow cytometry, gated on live singlet cells. (**B**) Within the CD27$^+$ memory gate, TLR stimulation expanded the proportion of IgM$^+$ cells relative to the mean of 49% for unstimulated cells. (**C**) Within the PC lineage committed CD27^{hi} gate, TLR stimulation expanded IgM$^+$ cells, unlike CD40L/IL-21. (B and C) Bars represent mean, and error bars represent SEM. (A) Representative figures from one donor out of four, with experiments performed in duplicate. (B and C) Summary of four independent donors with two replicates each. $^{\dagger}p < 0.1$, $^{***}p < 0.001$. CS, class-switched defined as IgM$^-$.

Culture and stimulation conditions

Agonists included a TLR7 agonist imidazoquinoline compound (Clo97), used at 250 ng/ml, and a TLR9 CpG-B agonist (ODN2006), used at 300 ng/ml (Invivogen, San Diego, CA). Additional TLR cultures included IFN-α at 1000 U/ml (Schering, Kenilworth, NJ) to maximize TLR responses (5). To mimic T follicular helper cell activation, we cultured B cells with 150 ng/ml trimerized recombinant human CD40L (Enzo Life Sciences, Farmingdale, NY) in conjunction with 10 ng/ml recombinant human IL-21 (Cell Signaling, Danvers, MA) (16). Culture media consisted of RPMI 1640 (Cellgro, Herndon, VA) supplemented with 10% inactivated FBS (Atlanta Biologicals, Lawrenceville, GA), 1% L-glutamine, HEPES, and antibacterial/antimycotic supplements (Life Technologies, Grand Island, NY). Cells were cultured

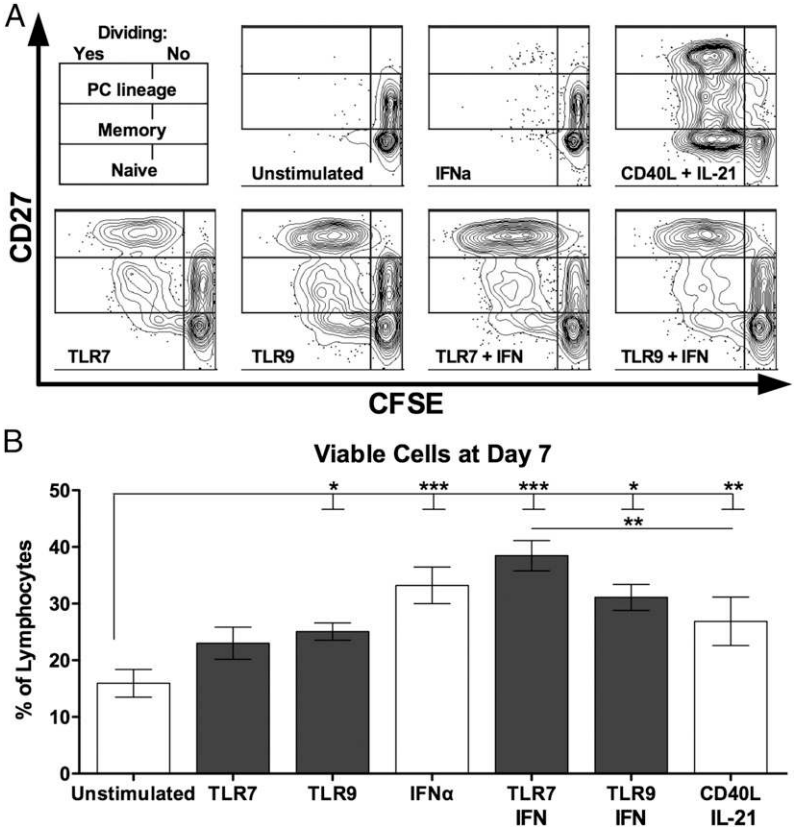

FIGURE 2. CD40L/IL-21 promotes proliferation of most B cells, whereas TLR stimulation is selective. (**A**) Representative day 7 cultured cells characterized by flow cytometry, gated on live singlet cells. (**B**) The proportion of live cells did not differ among stimuli at day 7. Bars represent mean, and error bars represent SEM. (A) Representative figures from one donor out of two, with experiments performed in duplicate. (B) Summary of four independent donors with two replicates each. $^{*}p < 0.05$, $^{**}p < 0.01$, $^{***}p < 0.001$.

in either U-bottom 96-well plates at a density of 1×10^5 in 200 μl, or in 24-well plates at a density of 1.15×10^6 in 1 ml (BD Biosciences, San Jose, CA). To assess proliferation, we stained B cells at baseline with CellTrace CFSE (Life Technologies, Grand Island, NY) as per manufacturer's instructions and cultured for 7 d in 96-well plates as described earlier.

Flow cytometry

B cells were Fc blocked (BD Biosciences) before staining. Cells were analyzed using an LSR Fortessa cytometer (BD Biosciences), with gating performed by first setting a wide lymphocyte gate by forward and side scatter, followed by two sets of doublet exclusion, first by forward scatter (FSC)–area by FSC-height and then by FSC-area by FSC-width, and by excluding dead cells with a viability stain (Life Technologies, Grand Island, NY). B cell purity was determined during isolation and at baseline by staining for CD19 (clone HIB19; eBioscience, San Diego, CA). Cell phenotype was determined by staining IgM (clone MHM-88), CD27 (clone O323), and CD38 (clone HIT2; all from BioLegend, San Diego, CA), with results reported for the live cells gate. B cell proliferation was determined by dilution of CFSE dye, with results reported for the live singlet lymphocyte gate.

Ig quantification

Total IgM and IgG levels in culture supernatants were quantified by ELISA (Bethyl Laboratories, Montgomery, TX), developed with TMB (BD Biosciences), stopped using 2N sulfuric acid (Sigma-Aldrich, St. Luis, MO), and read using the uQuant Microplate Reader (Bio-Tek, Winooski, VT).

HEp-2 staining

Thirty microliters of undiluted culture supernatants were tested for presence of autoreactive Abs using HEp-2 slides and immunofluorescence reagents as per manufacturer's instructions (MBL, Des Plaines, IL) for total Ig detection. A second slide was tested for IgM-specific Abs with FITC-conjugated anti-human IgM (Dako, Glostrup, Denmark). Vectashield hardset mounting media (Vector Labs, Burlingame, CA) was used to prevent photobleaching while slides were read on an Axioplan 2 microscope (Zeiss, Jena, Germany). Interpretation of staining patterns was carried out based on descriptions provided by MBL in the product documentation.

IgH deep sequencing

Genomic DNA was isolated via centrifugation-based purification (ArchivePure; 5Prime, Hamburg, Germany), and 1 μg (one donor) or 2 μg (three donors) DNA was frozen for survey-depth sequencing of the IgH locus (Adaptive Biotechnologies, Seattle, WA). Adaptive Biotechnologies performed the library generation, deep sequencing, and sequence filtering. The sequences obtained were processed with IMGT (17) to assign IgHV, IgHD, and IgHJ genes, delimit CDR3 boundaries, and annotate somatically hypermutated nucleotides. From 1 μg DNA from 1 donor, between 9,306 and 24,660 unique productive sequences were obtained (mean, 17,335), whereas the other 3 donors had 17,500 to 70,500 unique productive sequences obtained from 2 μg DNA (mean 31,645). Total productive reads per sample ranged from 200,000 to 1,500,000 (mean, 679,334). Sequences that could not be assigned to IgHV and IgHJ families were not considered in the analyses, whereas those predicted to have stop codons or frame shifts were used as false discovery internal controls.

Sequence analysis

SHM status was determined by mutations in the IgHV gene, with a mutated sequence being defined as containing two or more mutations to avoid potential mislabeling caused by PCR artifacts. The IgHV gene was selected because it contains the most nucleotides, and thus has the highest correct alignment probability in various alignment algorithms including IMGT (18). Analysis was performed using the programming language R (19), using the RStudio wrapper (20) and the plyr (21), stringr, ggplot2 (22), gplots, RColorBrewer, reshape (23), cluster (24), Interpol, and data.table packages. Unless otherwise indicated, analysis was performed on unique sequences to eliminate any bias arising from selective sequence amplification during sequencing. Although PCR amplification might introduce such bias, the proprietary sequencing and filtering method used by Adaptive Biotechnologies corrects for PCR bias (25), thereby minimizing this concern. As such, differential impacts of stimulation on cell proliferation can be assessed by factoring in relative sequence frequencies because these are proportional to the number of input B cells bearing a given rearrangement in genomic DNA-based sequencing.

Statistics

Statistical tests were performed in R or in Prism (Version 5; GraphPad, San Diego, CA). Results were first assessed by repeated-measures ANOVA, with Dunnett's multiple comparison tests as post hoc, using the unstimulated samples as controls. For differentiation and Ig secretion, additional post hoc testing, with Dunnett's tests, was performed to compare results with CD40L/IL-21 treatment. With the exception of B differentiation and Ig secretion, following a significant ANOVA, samples were normalized to unstimulated samples by subtraction to directly assess the impact of stimulation while controlling for nonspecific effects of culture and for baseline differences between donors. Normalized results were tested with one-sample *t* tests versus the hypothetical mean of 0 to determine whether treatment led to any changes. Clustering was performed based on Euclidean distances and complete clustering using the heatmap.2 function from the gplots package. Given the potential for false discovery with any study of large data sets, identical analysis was performed on the unproductive sequence subset. Such sequences are bystanders, unshaped by selection and subject to expansion or contraction based on the independent productive rearrangement present in the same cell. Changes observed with TLR stimulation, such as gene usage and CDR3 charge and length characteristics, are not expected in these sequence repertoires. Changes relating to SHM, meanwhile, are expected to appear because activation-induced cytosine deaminase, the enzyme mediating SHM, induces mutations whenever the Ig locus is transcribed, which also occurs for nonproductive rearrangements. All findings re-

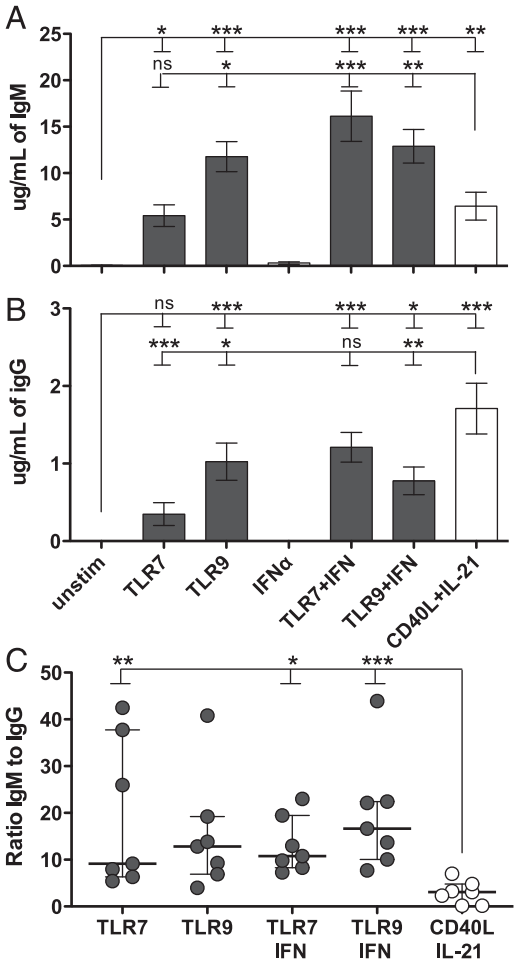

FIGURE 3. TLRs skews Ab secretion toward IgM. (**A**) TLR9 and TLR/IFN-stimulated cells secreted high levels of IgM. (**B**) Stimulated B cells also secreted IgG, with CD40L/IL-21 inducing more robust secretion. (**C**) TLR stimulation skewed responding B cells toward secreting higher levels of IgM relative to IgG. (A and B) Bars represent mean, and error bars represent SEM. (C) Bar represents median, and error bars represent interquartile range. Summary of four independent donors with two replicates each. ns, $p > 0.1$, $*p < 0.05$, $**p < 0.01$, $***p < 0.001$.

ported follow these patterns, with results deviating from these patterns deemed to represent artifacts and excluded.

Results

TLR stimulation expands IgM$^+$ memory, IgM$^+$ PC committed, and IgM-secreting B cells

Peripheral blood B cells (>97% pure) of each donor were cultured with TLR7 and TLR9 agonists, with or without IFN-α, or, for comparison, CD40/IL-21, to assess the relative frequencies of responding B cell populations. All stimulation conditions successfully induced B cell differentiation into CD27^{hi} cells committed to the PC lineage (Fig. 1A, representative donor). The pattern of responses differed, however, with TLRs selectively expanding the proportion of IgM$^+$ B cells among CD27$^+$ memory populations (ANOVA $p < 0.01$; Fig. 1B), represented as the change in proportion of IgM$^+$ cells in the memory gate to control for baseline differences between donors. Similarly, TLRs selectively promoted IgM$^+$ B cells and among CD27^{hi} populations (ANOVA $p < 0.0001$; Fig. 1C). CD40L/IL-21 stimulation, however, showed no selectivity among memory populations and favored differentiation into class-switched IgM$^-$ CD27^{hi} cells. Similarly, although all stimuli induced B cell proliferation, the patterns of proliferation were different (Fig. 2A, representative donor). Whereas CD40L/IL-21 induced proliferation of virtually all memory B cells and of a majority of naive B cells, TLRs induced only a subset of these cells to divide. TLR-responsive B cells, however, showed further dilution of CFSE, indicating more rounds of cell division. Despite the different proliferative responses, the proportion of live cells was largely similar among stimulated cells at the end of the culture (Fig. 2B), as were the cell counts (data not shown).

Both TLRs and CD40L/IL-21 robustly induced secretion of IgM (ANOVA $p < 0.0001$; Fig. 3A), and IgG was similarly secreted (ANOVA $p < 0.0001$; Fig. 3B). Notably, TLRs heavily skewed secretion toward IgM, whereas CD40L/IL-21 stimulation fostered relatively more balanced IgM and IgG production (ANOVA $p = 0.0037$; Fig. 3C).

Deep sequencing of the IgH locus reveals clustering of TLR-stimulated cells based on V and J usage

To examine whether TLR-responsive B cells showed similar BCR structure, we performed deep sequencing of the IgH locus of these cells to compare with those cultured with CD40L/IL-21. Fig. 4A shows that, among mutated sequences, TLR9 and TLR/IFN-stimulated cells from four donors shared similar changes in IgHV to IgHJ rearrangement frequencies, segregating these responders apart from CD40L/IL-21–stimulated and control cells. Similar clustering was obtained from repertoires that included nonmutated sequences, whereas clustering was weaker for repertoires of only nonmutated sequences (data not shown). Analysis of BCR composition changes showed that TLR stimulation selectively ex-

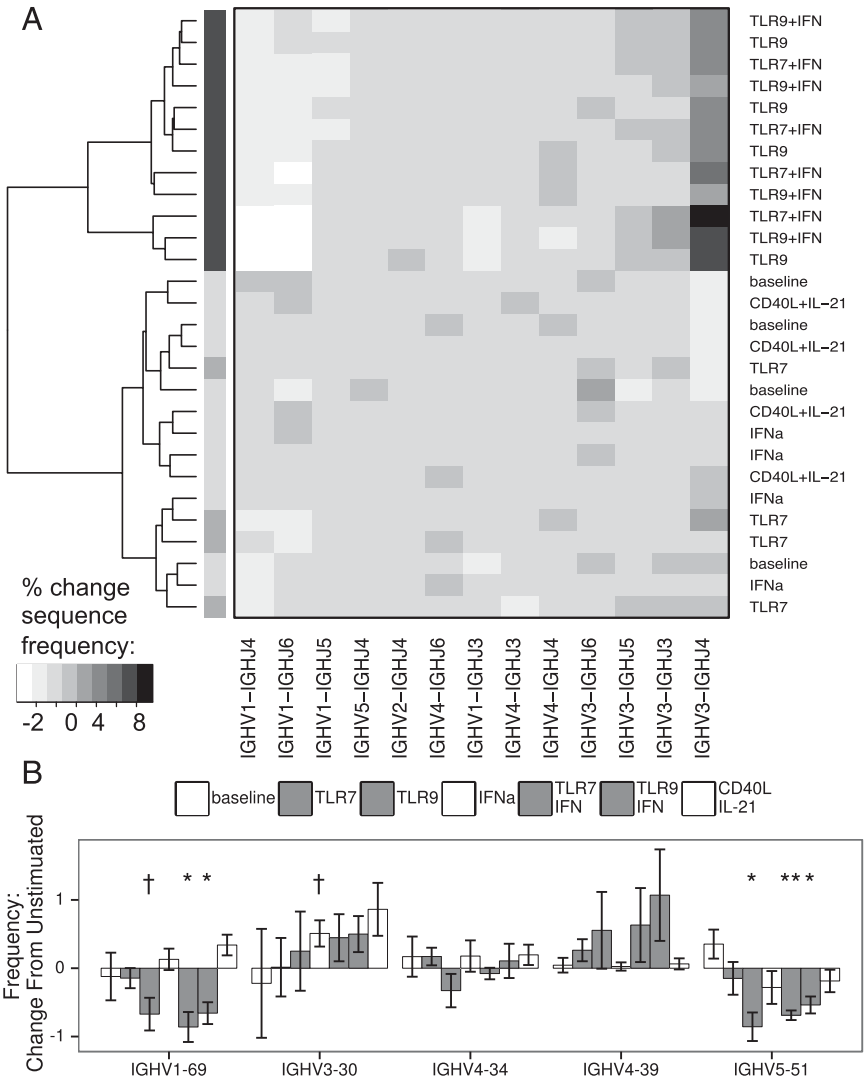

FIGURE 4. Deep sequencing of the IgH locus reveals clustering of TLR-stimulated cells based on V and J usage. (**A**) Unbiased clustering of IgHV and IgHJ pairing frequencies of the mutated sequence subset, showing grouping of TLR9 and TLR/IFN stimulated samples from four donors in contrast with other cultures (dendrogram shading added for ease of viewing). To control for interdonor differences and nonspecific changes due to culture, we normalized data based on unstimulated samples before clustering. (**B**) Changes in frequency of IgHV genes of specific interest (see *Results* for description). (A) Algorithm: complete clustering based on Euclidean distances for IgHV-IgHJ pairings, filtered on pairings with at least 1% change in frequency between any two samples. (B) Bars represent mean, and error bars represent SEM. Columns appear in order of legend. Data represent four independent donors, split across two independent sequencing runs. $^{\dagger}p < 0.1$, $^{*}p < 0.05$, $^{**}p < 0.01$.

panded B cells bearing V3-J1, V3-J3, V3-J4, V3-J5, and V6-J4 rearrangements, at the expense of B cells bearing V1-J2, V1-J3, V1-J4, V1-J5, and V5-J4 rearrangements (Supplemental Table I). CD40L/IL-21 stimulation, in contrast, expanded B cells bearing V1-J6 and V2-J6 rearrangements, but otherwise the repertoire did not differ from baseline B cells. Comparing sequences between donors also revealed that TLR stimulation, but not CD40L/IL-21, promoted expansion of B cells using similar IgHV genes (Supplemental Table II).

This analysis highlights the impact of stimulation on cell survival as each rearrangement, regardless of its relative frequency, was given equal weight. When these analyses were corrected for relative sequence frequencies, thereby factoring in survival and proliferation, the changes in BCR composition promoted by TLR9 and TLR/IFN stimulation again clustered apart from sequences derived from both CD40L/IL-21–stimulated and control cells (data not shown).

Changes in some IgHV genes have been reported to have associations with B cell subsets or functional outcomes. In particular, V1-69 was found in broadly neutralizing Abs to influenza cloned from IgM^+ memory B cells (26), and is overrepresented in nonmutated rearrangements in chronic lymphocytic leukemia (27). V3-30 has been found to be overrepresented in B cells class-switched to IgD (28) and has been associated with good prognosis in chronic lymphocytic leukemia (29). V4-34 has been shown to have autoimmune associations, particularly recognizing RBC Ags (30), whereas V4-39 was overrepresented in rotavirus-specific IgA and IgM PCs isolated from the gastrointestinal mucosa (31). Lastly, rearrangements involving V5-51 were common in IgA PCs recognizing tissue transglutaminase in the gastrointestinal mucosa of patients with celiac disease (32). When these IgHV genes were examined in this study, TLR activation was found to decrease the relative frequencies of B cells using V1-69 and V5-51, whereas CD40L/IL-21 did not show such an association (Fig. 4B, mutated repertoire; Supplemental Fig. 1, nonmutated and total repertoires). Other IgHV genes were altered as per Supplemental Table II.

The IgH locus shows convergent BCR composition after TLR stimulation

Because the CDR3 is the most variable portion of the IgH and is essential for Ag recognition (33), we then determined the influence of TLR and CD40/IL-21 signals on promoting sharing of CDR3 sequences. For this, we examined equally sized subsets of the

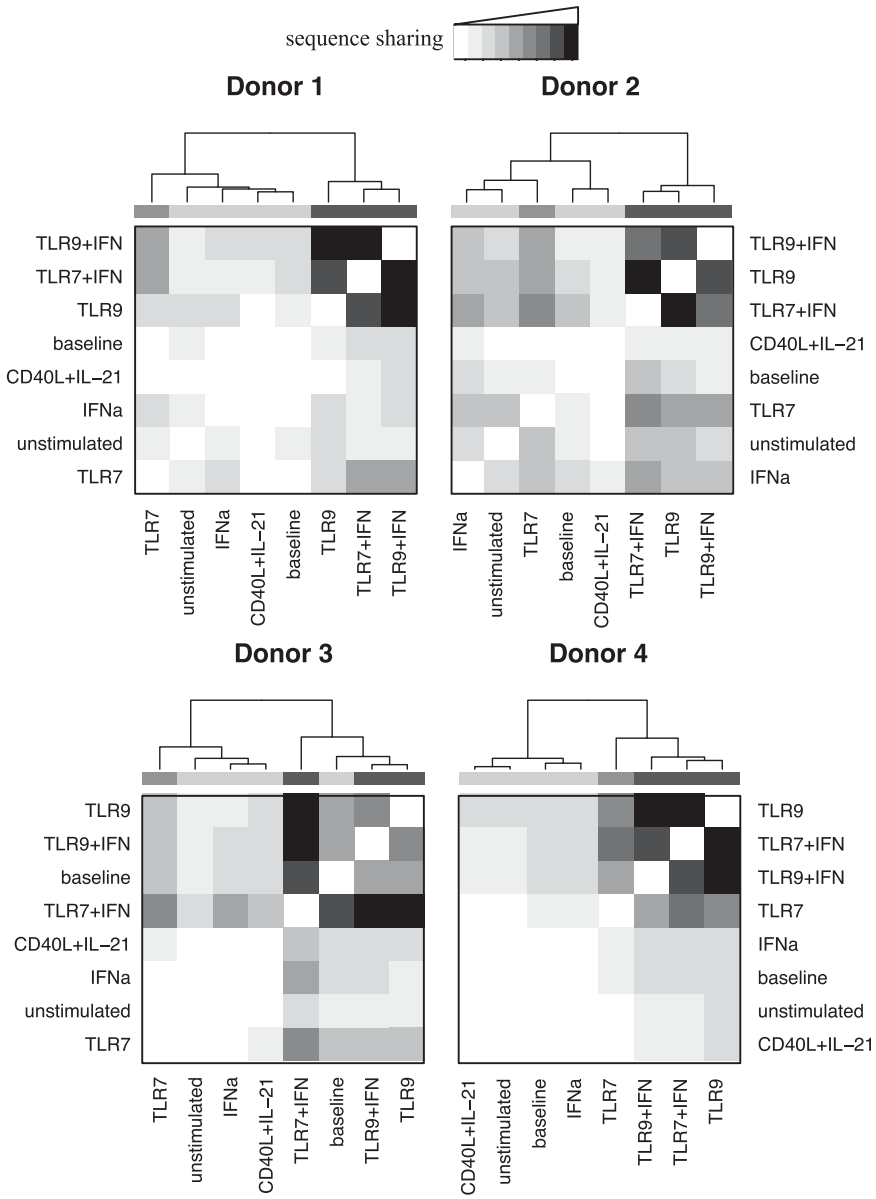

FIGURE 5. Deep sequencing of the IgH locus shows convergence of BCRs after TLR stimulation. TLR9 and TLR/IFN-activated B cells of each donor demonstrated increased CDR3 amino acid sequence sharing after stimulation, whereas two similarly showed convergence after TLR7 stimulation (sequence sharing as indicated). To control for differing sequencing depth, we examined repertoire subsets of equal size pairwise for all samples from each donor, counting overlapping sequences. These counts were then clustered based on complete clustering of Euclidean distances, with dendrogram shading added for ease of viewing. The greatest extent of overlap represents 0.5, 3.9, 3.3, and 1.75% sharing of sequences for donors 1–4. Data represent four independent donors, split across two independent sequencing runs, with subsampling performed five times.

overall repertoire for each donor for each condition. After either TLR9 or TLR/IFN stimulation, B cell cultures of individual donors shared up to 4% of their sequences (Fig. 5). In contrast, CD40L/IL-21 B cell activation did not induce CDR3 sharing, instead promoting proliferation of separate B cell populations. Patterns of sequence sharing were recapitulated when relative sequence frequencies were factored in (data not shown). These findings suggest that TLR stimuli activate similar B cells, leading to survival or expansion of cells that might be expected to produce Abs with similar Ag specificities. Although individuals shared specific rearrangements, we point out that sharing of identical sequences between donors was minimal, likely because of the vast sequence diversity at baseline.

Somatically hypermutated sequences expand after TLR stimulation

The sequence similarity induced by TLR stimulation suggests that some B cells might respond to TLR activation more strongly than others, unlike B cells activated by CD40L/IL-21. To characterize these differences, we first examined patterns of SHM, defined as two or more mutations in the IgHV nucleotide sequence. TLR stimulation increased the proportion of mutated sequences, whereas CD40L/IL-21 stimulation did not (Fig. 6), with similar findings obtained when considering relative sequence frequency. Among mutated sequences, however, the extent of mutation was not significantly affected by any stimulation, both when assessed per donor or per IgHV family (data not shown). As such, TLR stimulation likely expanded B cells that were mutated at baseline.

TLR stimulation expands B cells bearing shorter and less negatively charged CDR3 segments

Because of its importance for Ag recognition, the construction of the CDR3 was assessed. We noted that the mean CDR3 length decreased for TLR9 and TLR/IFN-stimulated B cells, whereas CD40L/IL-21 stimulation failed to induce length changes. These TLR-induced changes were entirely contained within the mutated sequence subset where, on average, half of a codon was lost from the mean length of 15.3 residues (Fig. 7A). When relative sequence frequencies were considered, the CDR3 segments of mutated sequences from TLR9 and TLR/IFN-stimulated cells were shortened by two thirds of a codon from a mean of 15.3 residues. To better understand these differences, we examined frequency distributions of CDR3 lengths of mutated sequences, revealing an expansion of shorter CDR3 segments after TLR stimulation that was not seen after treatment with CD40L/IL-21 (Fig. 7B). Similar changes were not consistently found among the nonmutated sequence repertoires (Supplemental Fig. 2).

TLR9 and TLR/IFN stimulation also expanded B cells bearing less negatively charged CDR3 segments (Fig. 8A, nonmutated, and Fig. 8B, mutated subset). The TLR-induced changes would be

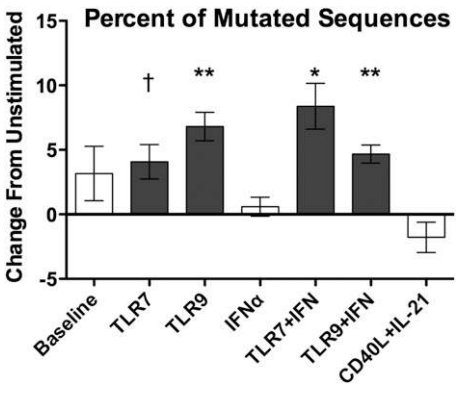

FIGURE 6. TLR stimulation expands mutated B cells. The proportion of somatically hypermutated sequences (2+ IgHV mutations) increased with TLR stimulation relative to mean proportion of 25% for unstimulated cells. CD40L/IL-21 stimulation did not change the proportion of mutated sequences. Plot indicates data normalized intradonor to unstimulated cultures. Bars represent mean, and error bars represent SEM. Data represent four independent donors, split across two independent sequencing runs. $^{\dagger}p < 0.1$, $*p < 0.05$, $**p < 0.01$.

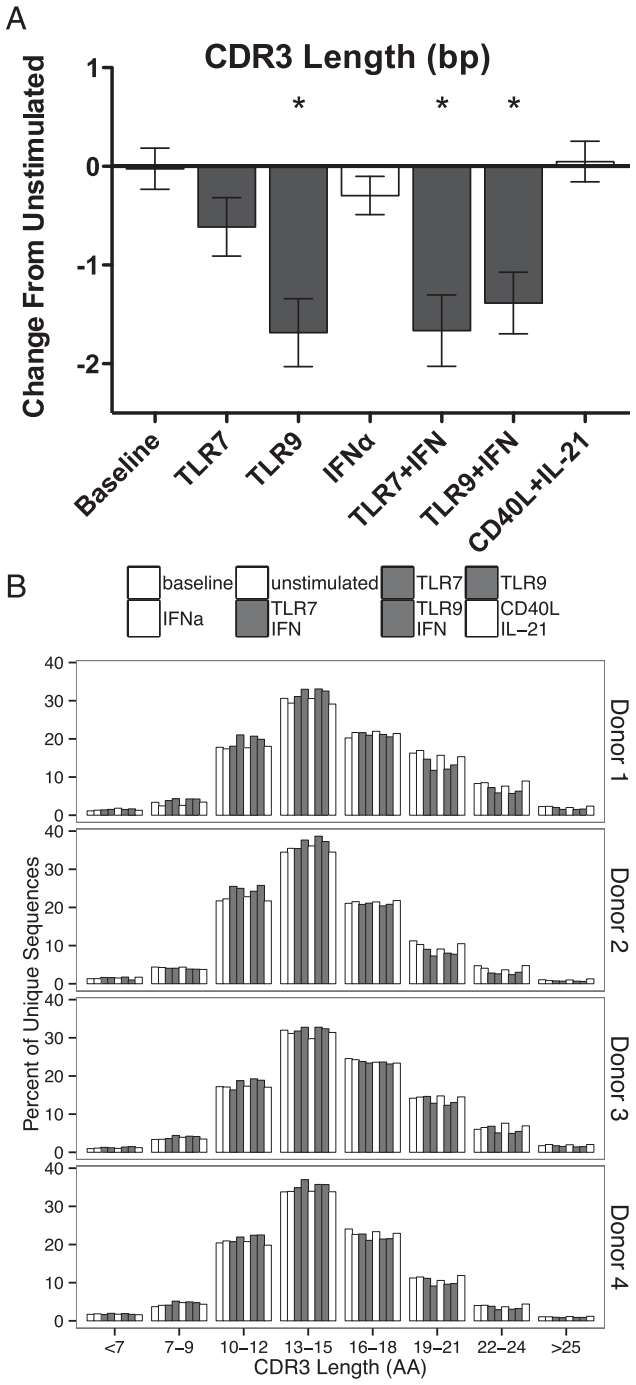

FIGURE 7. TLR stimulation expands cells bearing shorter CDR3 segments. (**A**) TLR stimulation selectively expanded B cells with shorter CDR3 segments, particularly among mutated B cells, relative to mean length of 46 bases for unstimulated cells. (**B**) TLR stimulation shifts the frequency distribution of CDR3 lengths toward shorter CDR3s. (A) Bars represent mean, and error bars represent SEM. (B) Bars represent sum of the proportion of unique sequences with a CDR3 length in the indicated length range. Columns appear in order of legend. Data represent four independent donors, split across two independent sequencing runs. $*p < 0.05$.

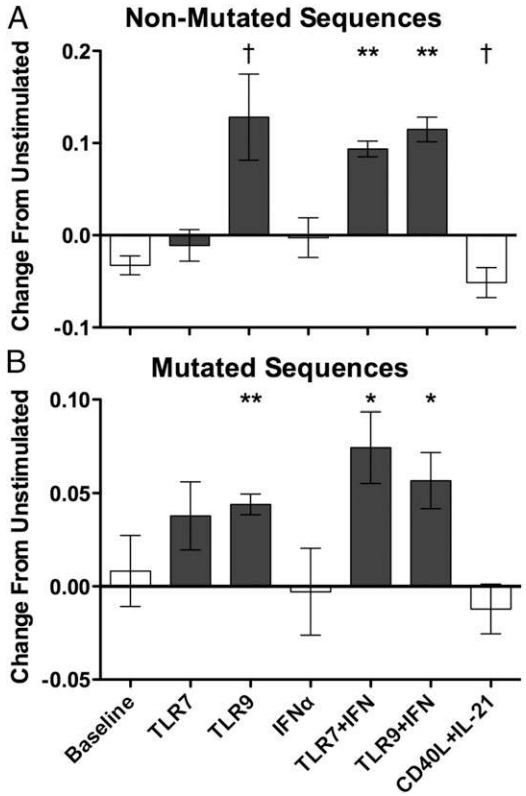

FIGURE 8. TLR stimulation expands cells bearing less negatively charged CDR3 segments. TLR9 and TLR/IFN stimulation induced less negatively charged CDR3 segments in both nonmutated (**A**) and mutated (**B**) sequence subsets relative to mean charges of −0.55 and −0.47 for unstimulated cells. Bars represent mean. Error bars represent SEM. Data represent four independent donors, split across two independent sequencing runs. $^{\dagger}p < 0.1$, $^{*}p < 0.05$, $^{**}p < 0.01$.

likely to impact Ag recognition because they represented large percent increases relative to the mean charge of unstimulated cells, with increases of 37–63% for unique sequences and increases of 45–80% when considering relative sequence frequencies. In contrast, CD40L/IL-21 stimulation weakly promoted increasingly negative charges in nonmutated B cells, trending toward an average reduction of 23% relative to the mean charge of unstimulated cells. To better understand these changes, we determined the proportions of sequences bearing specific CDR3 charges, revealing TLR-driven expansion of B cells bearing CDR3s with net charges of 1 to 3 in nonmutated sequences, compared with CDR3s of net charge of 1 in mutated sequences (data not shown). As expected by the changes in charge, TLR stimulation decreased CDR3 acidic residues and increased CDR3 basic residues, with all amino acids in each group contributing to the differences (data not shown).

TLR stimulation induces CDR3 profiles consistent with antinuclear reactivity, as well as autoreactive Abs

For all cultures, longer CDR3 segments were more negatively charged than shorter CDR3s. Because TLR stimulation both shortened the CDR3 and increased the charge toward positive, we next assessed CDR3 charge among segments of equal length, finding that the magnitude of TLR-induced increase in charge was positively correlated with CDR3 length (Fig. 9A).

Longer and positively charged CDR3 segments have previously been associated with autoreactivity (34). Because TLR stimulation favored the emergence of such CDR3s, we tested whether the Abs secreted after stimulation bound to HEp-2 cells. Culture supernatants from TLR9 and TLR/IFN-stimulated cultures showed robust reactivity, unlike cultures activated by CD40L/IL-21 (Fig. 9B, representative images, and Fig. 9C, summary). Given the expansion noted in IgM^+ populations by flow cytometry, HEp-2 binding by IgM isotype Abs was specifically assessed, showing robust binding by Abs secreted after TLR9 and TLR/IFN stimulation (Fig. 9D). For both sets of slides, the strongest staining was cytoplasmic, consistent with tropomyosin or cytokeratin patterns, which overlaid a weaker nuclear staining consistent with centromere-associated proteins, nuclear matrix, MSA-2 midbody, or nuclear rim patterns.

Discussion

This study examined peripheral blood B cell responses of four donors to stimulation through TLR7 and TLR9, defining TLR-responsive B cells based on phenotype, Ig secretion, and BCR structure. In contrast with CD40L/IL-21 stimulation, TLRs expanded IgM^+ B cells from $CD27^+$ memory and $CD27^{hi}$ PC lineage committed populations (15). TLR activation drove responding cells primarily toward secretion of IgM, unlike CD40L/IL-21 stimulation that induced relatively more balanced IgM and IgG production. Perhaps contributing to this difference, CD40L/IL-21 induced proliferation of virtually all memory and most naive B cells, whereas TLRs induced proliferation of a subset of these cells. TLR-responsive B cells shared BCR structure, showing characteristic patterns of IgHV and IgHJ usage, particularly in mutated sequences. Given their history of SHM, these sequences likely originated from memory B cells, as shown in older studies of sorted cells (35). Stimulation through TLRs, but not CD40L/IL-21, also expanded shared CDR3 sequences, indicating that a common subset of B cells may have responded to these stimuli. TLR responding cells were more likely to have mutated BCRs, and had shorter CDR3 segments bearing less negative charge. Interestingly, the magnitude of the TLR-induced increase in charge correlated with CDR3 length, resulting in a more positive charge among longer CDR3 segments. Of note, these TLR effects were found for each donor, showing similar patterns and magnitudes of effect, suggesting that TLR stimulation may commonly drive the survival and proliferation of a subset of human B cells. In contrast, B cells stimulated with CD40L/IL-21, which also induced proliferation, differentiation, and Ig secretion, genetically resembled the unstimulated samples, indicating that TLR-induced changes are unique and are not general consequences of B cell activation.

Although stimulation through TLR7, especially at the low doses used, is a weak activator of B cells, we noted that TLR7 and TLR9 or TLR/IFN stimulation resulted in similar promotion of IgM^+ responses. As noted previously, responses to TLR7 stimulation were robust when the receptor levels were boosted by IFN-α (1), leading to responses resembling those noted for TLR9 stimulation.

Both TLR and CD40L/IL-21 stimulation are able to drive commitment into PC lineage and Ig secretion, yet TLR stimulation biased both processes toward the IgM isotype relative to activation by CD40L/IL-21. A high-dose TLR9 agonist, in conjunction with BCR ligation, was previously reported to favor IgM secretion (36), results that are expanded in this study to include IgM induction after low-dose stimulation solely through TLR9 or TLR7. This TLR skewing of responses toward IgM raises the possibility that TLR-responsive B cells could have special effector responses, such as complement fixation or mucosal protection, for which IgM is quite suitable.

We found that IgM memory B cells, a heterogeneous mix of circulating splenic marginal zone B cells (37) and B cells originating from both GC-dependent and GC-independent activation (38), were particularly responsive to TLR activation. In support, more than half of TLR-induced changes in IgHV gene usage

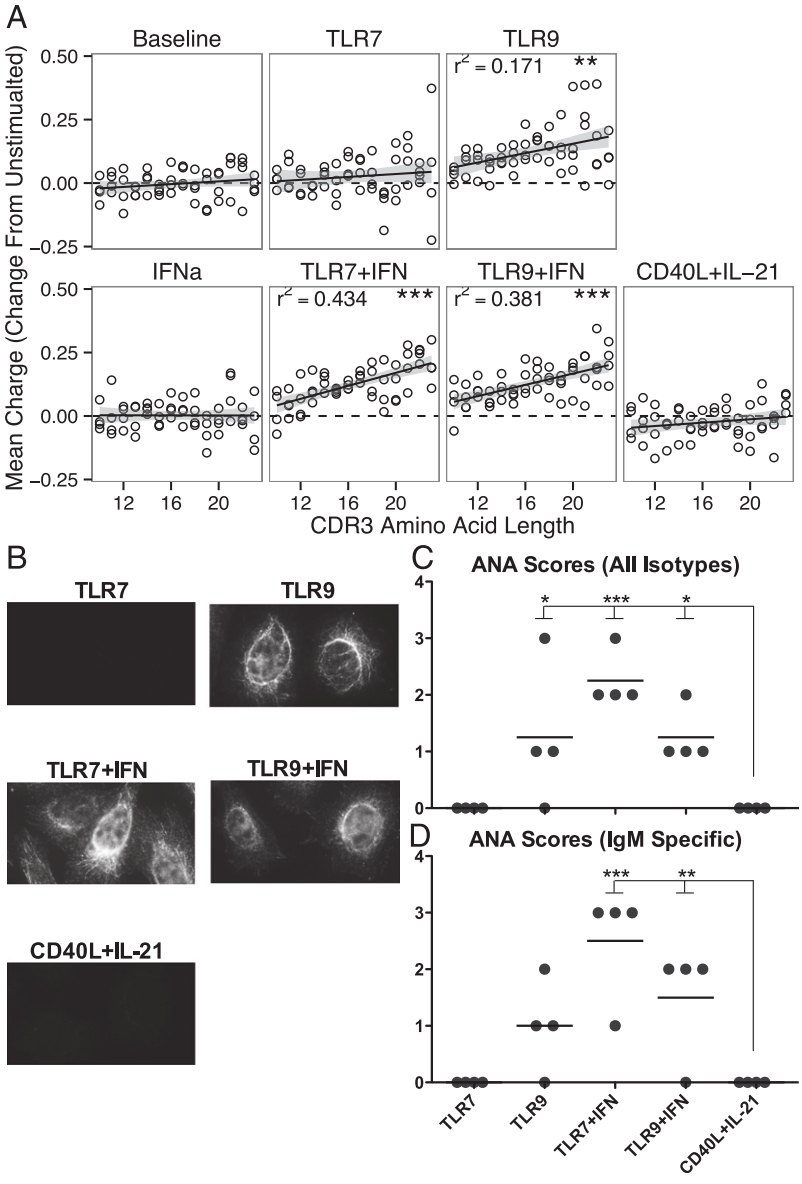

FIGURE 9. TLR stimulation induced autoreactive Abs. (**A**) TLR activation induced a mean charge increase that was positively correlated with CDR3 length. Plots indicate data normalized intradonor to unstimulated cultures, and CDR3 length range represents modal 90% of lengths. Gray line represents 95% confidence interval tracing for linear model and dotted black line as reference for no change. *r* refers to Pearson correlation coefficient. (**B**) Representative images obtained from probing culture supernatants for reactivity against HEp2 cells, showing induction of autoreactive Abs after TLR stimulation. Original magnification ×40. Summary of antinuclear staining scores for all donors using either anti–L chain (**C**) or anti-IgM isotype (**D**) detection reagents. Supernatant reactivity was graded on a scale of 0 (negative) or 1+ (weak staining) through 4+ (intense staining). (A) Data represent four independent donors, split across two independent sequencing runs. (B) Representative images from one donor. (C and D) Summary of four independent donors, each with two slides stained. $*p < 0.05$, $**p < 0.01$, $***p < 0.001$.

match previously published gene usage patterns found to differentiate IgM memory cells from naive or class-switched memory populations (39). IgM$^+$ memory B cells are potentially dependent on MyD88 signaling as patients with inborn errors in MyD88 and IRAK4 have reduced numbers of these cells (7, 40). The roles of endosomal TLR7 and TLR9 in promoting this subset are less clear, however, as two patients deficient in the TLR endosomal trafficker UNC93B1 had normal numbers of IgM$^+$ memory B cells, although these cells showed lower levels of SHM (40). Because TLR9 activation induced mutated IgM memory cells from cord-blood derived transitional B cells (41) and because we found TLRs to expand both IgM memory cells and mutated sequences, our data suggest that a mutated subset of IgM memory cells could be particularly responsive to endosomal TLRs, potentially explaining this reduction of IgM memory SHM in these few patients with UNC93B1 mutations.

Although TLRs clearly expand B cells bearing mutated BCRs, our results suggest expansion of B cells mutated at baseline over in vitro induction of mutations. Aranburu et al. (41) previously reported a TLR9-dependent induction of mutations in IgHV1 and IgHV4/6, but not IgHV5, in cord-blood–derived transitional B cells. In contrast, we found no IgHV-specific differences in extent of mutation in total B cell populations after TLR stimulation. Because the previous study assessed cells at an earlier stage of differentiation, used a higher concentration of TLR9 agonist in concert with BCR ligation, focused on proliferating cells, and sequenced single cells, the differences in results are perhaps not surprising. Although factoring in proliferation did not alter our results, it remains possible that de novo mutations were specifically introduced in dividing B cells. More likely, however, is that this difference reflects response patterns of adult peripheral blood B cells as opposed to cord blood B cells.

For each donor, TLR stimulation promoted positive charges among longer CDR3 segments, reminiscent of autoreactive Abs (34). Accordingly, we found that TLR activation promoted autoantibody secretion from B cells of these healthy individuals, findings previously described for autoimmune-prone mice (42–45) and humans with autoimmunity (46–48). Although roughly one fourth of healthy individuals have autoreactive Abs detectable in serum (49), in these experiments, TLR stimulation induced detectable autoantibodies in culture supernatants of all donors, including IgM isotype autoantibodies. These data were somewhat unexpected based on earlier reports that found IgG$^+$ memory B cells to have high rates of autoreactivity, whereas IgM$^+$ memory

populations had virtually none (50). There are, however, significant methodological differences between our study, where we assess the Abs secreted in response to stimulation, and earlier studies that examined the reactivity of Abs cloned from single B cells. As such, the difference in results is perhaps not surprising. Follow-up studies to assess the profile of Abs secreted by various B cell populations in response to TLR stimulation will be required to fully examine these differences.

As has been pointed out elsewhere, autoreactivity can also be protective, as is the case for many NAs that may ameliorate autoimmunity (51, 52) and help maintain homeostasis (51). IgM NAs are often positively charged to facilitate interaction with negatively charged targets (53), and may have high levels of polyreactivity (54). Murine B1 cells secreting NA are also TLR responsive (11, 55) and have unique BCR construction (56), making them distinct from pathogenic anti-nuclear autoantibody-producing cells (57). Because a human analog of B1 cells has not been definitively described (58–63), human NA-secreting B cells are not as well understood, although IgM memory B cells have been proposed as a source of these Abs (37, 64). Potentially, the TLR-responsive cells identified in this article are cells of this lineage despite the reduced frequencies of V1-69 noted after TLR stimulation.

The selectivity of TLR responsiveness among B cells has implications for the emerging field of TLR9-based vaccine adjuvants, as reviewed by Vollmer and Krieg (65) and Bode et al. (66). Developing such agonists has been actively pursued, both in mice (67) and in small phase I/II studies in humans (68, 69). In humans, TLR9 adjuvants both boosted and modulated the immune response, increasing IgG1 and IgG3, but reducing IgG4 responses in one report, and transiently elevating anti-DNA Abs in a few subjects in both reports (68, 69). Based on results presented in this article, TLR-based adjuvants might also drive secretion of Abs of additional, and potentially autoreactive, specificities; however, the extent to which TLR-responsive B cells could be directly activated in vivo by TLR adjuvants remains unclear. Closer study of TLR-responsive B cells and of Abs induced by TLR stimulation, both in vitro and in vivo, are needed to better understand the impact of such stimulation on human B cells.

Acknowledgments

We thank the staff of the Department of Scientific Computing (Icahn School of Medicine, Mount Sinai, New York, NY) for computational resources and expertise. Microscopy was performed at the Microscopy Shared Resource Facility (Icahn School of Medicine, Mount Sinai).

Disclosures

The authors have no financial conflicts of interest.

References

1. Bekeredjian-Ding, I. B., M. Wagner, V. Hornung, T. Giese, M. Schnurr, S. Endres, and G. Hartmann. 2005. Plasmacytoid dendritic cells control TLR7 sensitivity of naive B cells via type I IFN. *J. Immunol.* 174: 4043–4050.
2. Glaum, M. C., S. Narula, D. Song, Y. Zheng, A. L. Anderson, C. H. Pletcher, and A. I. Levinson. 2009. Toll-like receptor 7-induced naive human B-cell differentiation and immunoglobulin production. *J. Allergy Clin. Immunol.* 123: 224–230.e4.
3. He, B., X. Qiao, and A. Cerutti. 2004. CpG DNA induces IgG class switch DNA recombination by activating human B cells through an innate pathway that requires TLR9 and cooperates with IL-10. *J. Immunol.* 173: 4479–4491.
4. Bernasconi, N. L., N. Onai, and A. Lanzavecchia. 2003. A role for Toll-like receptors in acquired immunity: up-regulation of TLR9 by BCR triggering in naive B cells and constitutive expression in memory B cells. *Blood* 101: 4500–4504.
5. Giordani, L., M. Sanchez, I. Libri, M. G. Quaranta, B. Mattioli, and M. Viora. 2009. IFN-alpha amplifies human naive B cell TLR-9-mediated activation and Ig production. *J. Leukoc. Biol.* 86: 261–271.
6. Capolunghi, F., S. Cascioli, E. Giorda, M. M. Rosado, A. Plebani, C. Auriti, G. Seganti, R. Zuntini, S. Ferrari, M. Cagliuso, et al. 2008. CpG drives human transitional B cells to terminal differentiation and production of natural antibodies. *J. Immunol.* 180: 800–808.
7. Maglione, P. J., N. Simchoni, S. Black, L. Radigan, J. R. Overbey, E. Bagiella, J. B. Bussel, X. Bossuyt, J. L. Casanova, I. Meyts, et al. 2014. IRAK-4 and MyD88 deficiencies impair IgM responses against T-independent bacterial antigens. *Blood* 124: 3561–3571.
8. So, N. S., M. A. Ostrowski, and S. D. Gray-Owen. 2012. Vigorous response of human innate functioning IgM memory B cells upon infection by *Neisseria* gonorrhoeae. *J. Immunol.* 188: 4008–4022.
9. Gunn, K. E., and J. W. Brewer. 2006. Evidence that marginal zone B cells possess an enhanced secretory apparatus and exhibit superior secretory activity. *J. Immunol.* 177: 3791–3798.
10. Martin, F., A. M. Oliver, and J. F. Kearney. 2001. Marginal zone and B1 B cells unite in the early response against T-independent blood-borne particulate antigens. *Immunity* 14: 617–629.
11. Genestier, L., M. Taillardet, P. Mondiere, H. Gheit, C. Bella, and T. Defrance. 2007. TLR agonists selectively promote terminal plasma cell differentiation of B cell subsets specialized in thymus-independent responses. *J. Immunol.* 178: 7779–7786.
12. Fagarasan, S., N. Watanabe, and T. Honjo. 2000. Generation, expansion, migration and activation of mouse B1 cells. *Immunol. Rev.* 176: 205–215.
13. Gray, D., I. C. MacLennan, H. Bazin, and M. Khan. 1982. Migrant mu+ delta+ and static mu+ delta- B lymphocyte subsets. *Eur. J. Immunol.* 12: 564–569.
14. Oliver, A. M., F. Martin, and J. F. Kearney. 1999. IgMhighCD21high lymphocytes enriched in the splenic marginal zone generate effector cells more rapidly than the bulk of follicular B cells. *J. Immunol.* 162: 7198–7207.
15. Avery, D. T., J. I. Ellyard, F. Mackay, L. M. Corcoran, P. D. Hodgkin, and S. G. Tangye. 2005. Increased expression of CD27 on activated human memory B cells correlates with their commitment to the plasma cell lineage. *J. Immunol.* 174: 4034–4042.
16. Zotos, D., J. M. Coquet, Y. Zhang, A. Light, K. D'Costa, A. Kallies, L. M. Corcoran, D. I. Godfrey, K. M. Toellner, M. J. Smyth, et al. 2010. IL-21 regulates germinal center B cell differentiation and proliferation through a B cell-intrinsic mechanism. *J. Exp. Med.* 207: 365–378.
17. Alamyar, E., P. Duroux, M. P. Lefranc, and V. Giudicelli. 2012. IMGT(®) tools for the nucleotide analysis of immunoglobulin (IG) and T cell receptor (TR) V-(D)-J repertoires, polymorphisms, and IG mutations: IMGT/V-QUEST and IMGT/HighV-QUEST for NGS. *Methods Mol. Biol.* 882: 569–604.
18. Munshaw, S., and T. B. Kepler. 2010. SoDA2: a Hidden Markov Model approach for identification of immunoglobulin rearrangements. *Bioinformatics* 26: 867–872.
19. R Development Core Team. 2014. R: A Language and Environment for Statistical Computing. R Foundation for Statistical Computing, Vienna, Austria. ISBN 3-900051-07-0. Available at: http://www.R-project.org.
20. RStudio, Inc. 2012. RStudio: Integrated development environment for R. RStudio, Inc., Boston, MA. http://www.rstudio.com/about/eula/.
21. Wickham, H. 2011. The Split-Apply-Combine Strategy for Data Analysis. *J. Stat. Softw.* 40: 1–29. Available at: http://www.jstatsoft.org/v40/i01.
22. Wickham, H. 2009. *ggplot2: Elegant Graphics for Data Analysis*. Springer, New York.
23. Wickham, H. 2007. Reshaping data with the reshape package. *J. Stat. Softw.* 21: 1–29. Available at: http://www.jstatsoft.org/v21/i12.
24. Maechler, M., P. Rousseeuw, A. Struyf, M. Hubert, and K. Hornik. 2015. cluster: Cluster Analysis Extended. R package version 2.0.1. Available at: http://cran.r-project.org/web/packages/cluster/index.html.
25. Carlson, C. S., R. O. Emerson, A. M. Sherwood, C. Desmarais, M. W. Chung, J. M. Parsons, M. S. Steen, M. A. LaMadrid-Herrmannsfeldt, D. W. Williamson, R. J. Livingston, et al. 2013. Using synthetic templates to design an unbiased multiplex PCR assay. *Nat. Commun.* 4: 2680.
26. Throsby, M., E. van den Brink, M. Jongeneelen, L. L. Poon, P. Alard, L. Cornelissen, A. Bakker, F. Cox, E. van Deventer, Y. Guan, et al. 2008. Heterosubtypic neutralizing monoclonal antibodies cross-protective against H5N1 and H1N1 recovered from human IgM+ memory B cells. *PLoS ONE* 3: e3942.
27. Johnson, T. A., L. Z. Rassenti, and T. J. Kipps. 1997. Ig VH1 genes expressed in B cell chronic lymphocytic leukemia exhibit distinctive molecular features. *J. Immunol.* 158: 235–246.
28. Seifert, M., S. A. Steimle-Grauer, T. Goossens, M. L. Hansmann, A. Bräuninger, and R. Küppers. 2009. A model for the development of human IgD-only B cells: Genotypic analyses suggest their generation in superantigen driven immune responses. *Mol. Immunol.* 46: 630–639.
29. Dal-Bo, M., I. Del Giudice, R. Bomben, D. Capello, F. Bertoni, F. Forconi, L. Laurenti, D. Rossi, A. Zucchetto, G. Pozzato, et al. 2011. B-cell receptor, clinical course and prognosis in chronic lymphocytic leukaemia: the growing saga of the IGHV3 subgroup gene usage. *Br. J. Haematol.* 153: 3–14.
30. Thorpe, S. J., C. E. Turner, F. K. Stevenson, M. B. Spellerberg, R. Thorpe, J. B. Natvig, and K. M. Thompson. 1998. Human monoclonal antibodies encoded by the V4-34 gene segment show cold agglutinin activity and variable multireactivity which correlates with the predicted charge of the heavy-chain variable region. *Immunology* 93: 129–136.
31. Di Niro, R., L. Mesin, M. Raki, N. Y. Zheng, F. Lund-Johansen, K. E. Lundin, A. Charpilienne, D. Poncet, P. C. Wilson, and L. M. Sollid. 2010. Rapid generation of rotavirus-specific human monoclonal antibodies from small-intestinal mucosa. *J. Immunol.* 185: 5377–5383.
32. Di Niro, R., L. Mesin, N. Y. Zheng, J. Stamnaes, M. Morrissey, J. H. Lee, M. Huang, R. Iversen, M. F. du Pré, S. W. Qiao, et al. 2012. High abundance of plasma cells secreting transglutaminase 2-specific IgA autoantibodies with limited somatic hypermutation in celiac disease intestinal lesions. *Nat. Med.* 18: 441–445.
33. Xu, J. L., and M. M. Davis. 2000. Diversity in the CDR3 region of V(H) is sufficient for most antibody specificities. *Immunity* 13: 37–45.

34. Wardemann, H., S. Yurasov, A. Schaefer, J. W. Young, E. Meffre, and M. C. Nussenzweig. 2003. Predominant autoantibody production by early human B cell precursors. *Science* 301: 1374–1377.
35. Klein, U., K. Rajewsky, and R. Küppers. 1998. Human immunoglobulin (Ig)M+ IgD+ peripheral blood B cells expressing the CD27 cell surface antigen carry somatically mutated variable region genes: CD27 as a general marker for somatically mutated (memory) B cells. *J. Exp. Med.* 188: 1679–1689.
36. Poeck, H., M. Wagner, J. Battiany, S. Rothenfusser, D. Wellisch, V. Hornung, B. Jahrsdorfer, T. Giese, S. Endres, and G. Hartmann. 2004. Plasmacytoid dendritic cells, antigen, and CpG-C license human B cells for plasma cell differentiation and immunoglobulin production in the absence of T-cell help. *Blood* 103: 3058–3064.
37. Weller, S., M. C. Braun, B. K. Tan, A. Rosenwald, C. Cordier, M. E. Conley, A. Plebani, D. S. Kumararatne, D. Bonnet, O. Tournilhac, et al. 2004. Human blood IgM "memory" B cells are circulating splenic marginal zone B cells harboring a prediversified immunoglobulin repertoire. *Blood* 104: 3647–3654.
38. Berkowska, M. A., G. J. Driessen, V. Bikos, C. Grosserichter-Wagener, K. Stamatopoulos, A. Cerutti, B. He, K. Biermann, J. F. Lange, M. van der Burg, et al. 2011. Human memory B cells originate from three distinct germinal center-dependent and -independent maturation pathways. *Blood* 118: 2150–2158.
39. Wu, Y. C., D. Kipling, H. S. Leong, V. Martin, A. A. Ademokun, and D. K. Dunn-Walters. 2010. High-throughput immunoglobulin repertoire analysis distinguishes between human IgM memory and switched memory B-cell populations. *Blood* 116: 1070–1078.
40. Weller, S., M. Bonnet, H. Delagreverie, L. Israel, M. Chrabieh, L. Maródi, C. Rodriguez-Gallego, B. Z. Garty, C. Roifman, A. C. Issekutz, et al. 2012. IgM+IgD+CD27+ B cells are markedly reduced in IRAK-4-, MyD88-, and TIRAP- but not UNC-93B-deficient patients. *Blood* 120: 4992–5001.
41. Aranburu, A., S. Ceccarelli, E. Giorda, R. Lasorella, G. Ballatore, and R. Carsetti. 2010. TLR ligation triggers somatic hypermutation in transitional B cells inducing the generation of IgM memory B cells. *J. Immunol.* 185: 7293–7301.
42. Ehlers, M., H. Fukuyama, T. L. McGaha, A. Aderem, and J. V. Ravetch. 2006. TLR9/MyD88 signaling is required for class switching to pathogenic IgG2a and 2b autoantibodies in SLE. *J. Exp. Med.* 203: 553–561.
43. Celhar, T., R. Magalhães, and A. M. Fairhurst. 2012. TLR7 and TLR9 in SLE: when sensing self goes wrong. *Immunol. Res.* 53: 58–77.
44. Christensen, S. R., J. Shupe, K. Nickerson, M. Kashgarian, R. A. Flavell, and M. J. Shlomchik. 2006. Toll-like receptor 7 and TLR9 dictate autoantibody specificity and have opposing inflammatory and regulatory roles in a murine model of lupus. *Immunity* 25: 417–428.
45. Nickerson, K. M., S. R. Christensen, J. Shupe, M. Kashgarian, D. Kim, K. Elkon, and M. J. Shlomchik. 2010. TLR9 regulates TLR7- and MyD88-dependent autoantibody production and disease in a murine model of lupus. *J. Immunol.* 184: 1840–1848.
46. Chauhan, S. K., V. V. Singh, R. Rai, M. Rai, and G. Rai. 2013. Distinct autoantibody profiles in systemic lupus erythematosus patients are selectively associated with TLR7 and TLR9 upregulation. *J. Clin. Immunol.* 33: 954–964.
47. Laska, M. J., A. Troldborg, B. Hansen, K. Stengaard-Pedersen, P. Junker, B. A. Nexø, and A. Voss. 2014. Polymorphisms within Toll-like receptors are associated with systemic lupus erythematosus in a cohort of Danish females. *Rheumatology (Oxford)* 53: 48–55.
48. Mu, R., X. Y. Sun, L. T. Lim, C. H. Xu, C. X. Dai, Y. Su, R. L. Jia, and Z. G. Li. 2012. Toll-like receptor 9 is correlated to disease activity in Chinese systemic lupus erythematosus population. *Chin. Med. J. (Engl.)* 125: 2873–2877.
49. Wandstrat, A. E., F. Carr-Johnson, V. Branch, H. Gray, A. M. Fairhurst, A. Reimold, D. Karp, E. K. Wakeland, and N. J. Olsen. 2006. Autoantibody profiling to identify individuals at risk for systemic lupus erythematosus. *J. Autoimmun.* 27: 153–160.
50. Tiller, T., M. Tsuiji, S. Yurasov, K. Velinzon, M. C. Nussenzweig, and H. Wardemann. 2007. Autoreactivity in human IgG+ memory B cells. *Immunity* 26: 205–213.
51. Grönwall, C., J. Vas, and G. J. Silverman. 2012. Protective roles of natural IgM antibodies. *Front. Immunol.* 3: 66.
52. Mannoor, K., A. Matejuk, Y. Xu, M. Beardall, and C. Chen. 2012. Expression of natural autoantibodies in MRL-lpr mice protects from lupus nephritis and improves survival. *J. Immunol.* 188: 3628–3638.
53. Chikazawa, M., N. Otaki, T. Shibata, H. Miyashita, Y. Kawai, S. Maruyama, S. Toyokuni, Y. Kitaura, T. Matsuda, and K. Uchida. 2013. Multispecificity of immunoglobulin M antibodies raised against advanced glycation end products: involvement of electronegative potential of antigens. *J. Biol. Chem.* 288: 13204–13214.
54. Mannoor, K., Y. Xu, and C. Chen. 2013. Natural autoantibodies and associated B cells in immunity and autoimmunity. *Autoimmunity* 46: 138–147.
55. Gururajan, M., J. Jacob, and B. Pulendran. 2007. Toll-like receptor expression and responsiveness of distinct murine splenic and mucosal B-cell subsets. *PLoS ONE* 2: e863.
56. Tornberg, U. C., and D. Holmberg. 1995. B-1a, B-1b and B-2 B cells display unique VHDJH repertoires formed at different stages of ontogeny and under different selection pressures. *EMBO J.* 14: 1680–1689.
57. Reap, E. A., E. S. Sobel, P. L. Cohen, and R. A. Eisenberg. 1993. Conventional B cells, not B-1 cells, are responsible for producing autoantibodies in lpr mice. *J. Exp. Med.* 177: 69–78.
58. Descatoire, M., J. C. Weill, C. A. Reynaud, and S. Weller. 2011. A human equivalent of mouse B-1 cells? *J. Exp. Med.* 208: 2563–2564, author reply 2566–2569.
59. Perez-Andres, M., C. Grosserichter-Wagener, C. Teodosio, J. J. van Dongen, A. Orfao, and M. C. van Zelm. 2011. The nature of circulating CD27+CD43+ B cells. *J. Exp. Med.* 208: 2565–2566, author reply 2566–2569.
60. Griffin, D. O., N. E. Holodick, and T. L. Rothstein. 2011. Human B1 cells in umbilical cord and adult peripheral blood express the novel phenotype CD20+ CD27+ CD43+ CD70-. *J. Exp. Med.* 208: 67–80.
61. Reynaud, C. A., and J. C. Weill. 2012. Gene profiling of CD11b^{+} and CD11b^{-} B1 cell subsets reveals potential cell sorting artifacts. *J. Exp. Med.* 209: 433–434, author reply 434–436.
62. Tangye, S. G. 2013. To B1 or not to B1: that really is still the question! *Blood* 121: 5109–5110.
63. Covens, K., B. Verbinnen, N. Geukens, I. Meyts, F. Schuit, L. Van Lommel, M. Jacquemin, and X. Bossuyt. 2013. Characterization of proposed human B-1 cells reveals pre-plasmablast phenotype. *Blood* 121: 5176–5183.
64. Cerutti, A., M. Cols, and I. Puga. 2013. Marginal zone B cells: virtues of innate-like antibody-producing lymphocytes. *Nat. Rev. Immunol.* 13: 118–132.
65. Vollmer, J., and A. M. Krieg. 2009. Immunotherapeutic applications of CpG oligodeoxynucleotide TLR9 agonists. *Adv. Drug Deliv. Rev.* 61: 195–204.
66. Bode, C., G. Zhao, F. Steinhagen, T. Kinjo, and D. M. Klinman. 2011. CpG DNA as a vaccine adjuvant. *Expert Rev. Vaccines* 10: 499–511.
67. Gungor, B., F. C. Yagci, G. Tincer, B. Bayyurt, E. Alpdundar, S. Yildiz, M. Ozcan, I. Gursel, and M. Gursel. 2014. CpG ODN nanorings induce IFNα from plasmacytoid dendritic cells and demonstrate potent vaccine adjuvant activity. *Sci. Transl. Med.* 6: 35ra61.
68. Cooper, C. L., H. L. Davis, M. L. Morris, S. M. Efler, M. A. Adhami, A. M. Krieg, D. W. Cameron, and J. Heathcote. 2004. CPG 7909, an immunostimulatory TLR9 agonist oligodeoxynucleotide, as adjuvant to Engerix-B HBV vaccine in healthy adults: a double-blind phase I/II study. *J. Clin. Immunol.* 24: 693–701.
69. Cooper, C. L., H. L. Davis, J. B. Angel, M. L. Morris, S. M. Elfer, I. Seguin, A. M. Krieg, and D. W. Cameron. 2005. CPG 7909 adjuvant improves hepatitis B virus vaccine seroprotection in antiretroviral-treated HIV-infected adults. *AIDS* 19: 1473–1479.